The surface band structure of β-Ga_2O_3

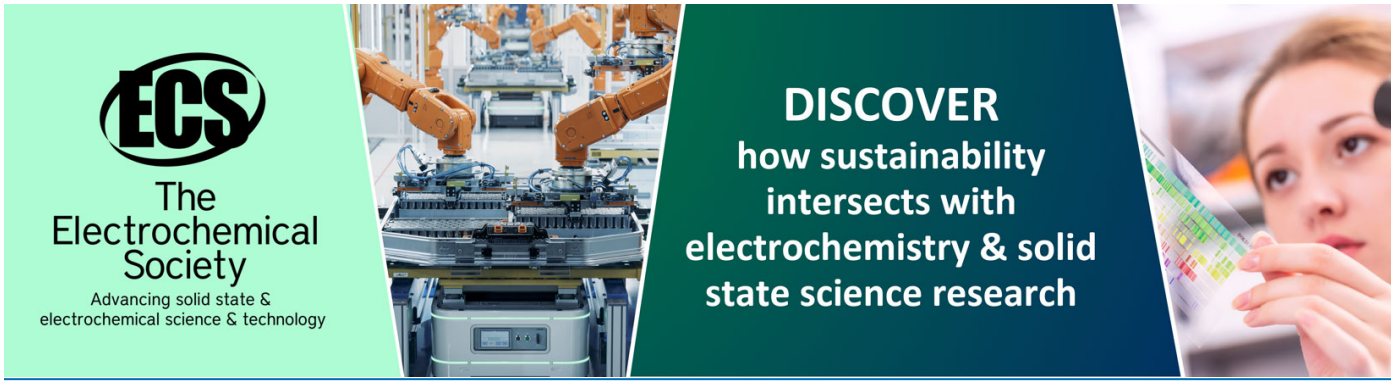

The surface band structure of β-Ga_2O_3

M Mohamed [1], I Unger, C Janowitz [1], R Manzke [1], Z Galazka [2], R Uecker [2] and R Fornari [2]

[1] Humboldt-Universität zu Berlin, Institut für Physik, Newtonstr. 15, 12489 Berlin, Germany
[2] Leibniz-Institut für Kristallzüchtung, Max-Born-Str. 2, 12489 Berlin, Germany

mansour@physik.hu-berlin.de

Abstract. Ga_2O_3 belongs to the group of transparent conducting oxides (TCOs) with a wide band gap and electrical conductivity. It exhibits the largest band gap with E_g = 4.8 eV and thus a unique transparency from the visible into the UV region. The information on the electronic structure of β-Ga_2O_3 is very scarce. This is in part due to the challenging problem of growing high purity single crystals. Transparent semiconducting β-Ga_2O_3 single crystals were grown by the Czochralski method from an iridium crucible under a dynamic protective atmosphere to control partial pressures of volatile species of Ga_2O_3. The investigated samples were characterized by different techniques (LEED, Laue, and STM). The experimental valence band structure of the of β-Ga_2O_3 single crystals along Γ-Z and A-M symmetry directions of the (100)-surface of Brillouin zone was determined by high-resolution angle-resolved photoelectron spectroscopy (ARPES) utilizing synchrotron radiation. The experimental band structure is compared and discussed with the theoretical calculations. The effect of changing the temperature from 300K to 20K on the experimental band structure β-Ga_2O_3 was studied.

1. Introduction

β-Ga_2O_3 is a large band gap semiconductor with the largest band gap of about 4.4–4.8 eV [1,2] among transparent conducting oxides (TCOs). Because β-Ga_2O_3 has a unique transparency from the visible into the UV region, it is a very promising candidate for optoelectronic devices operating at short wavelength [3], where the other TCOs have poor transparency. The electrical conductivity of β-Ga_2O_3 is attributed to the existence of oxygen vacancies. The amount of oxygen vacancies induced depends on the growth atmosphere [4,5]. The oxygen vacancies serve as shallow donors with an ionization energy of 0.03- 0.04 eV [6]. At high temperatures the oxygen vacancies concentration depends on the partial pressure of the atmosphere. Therefore, β-Ga_2O_3 is also a promising candidate for high temperature oxygen sensor applications [7]. Ga_2O_3 exhibits polymorphism, and five crystalline modifications have been reported: α, β, γ, δ and ε [8,9]. Of these, β-Ga_2O_3 is the only stable crystalline modification in the range from room temperature up to the melting point of about 1800 °C. All other polymorphs are metastable and transform to the β form at sufficiently high temperature [8]. Additionally, β-Ga_2O_3 has great chemical stability, being unaffected even by concentrated acids such as hydrofluoric acid [1]. β-Ga_2O_3 belongs to the space group C/2m, and its base-centered monoclinic lattice has unit cell parameters a = 12.23, b = 3.04, c = 5.80 and β = 103.7° [10, 11]. The b-axis of the

centrosymmetric unit cell is the twofold rotational axis, and the mirror plane (i.e., the (010)) is perpendicular to this axis. There are four Ga_2O_3 units per crystallographic unit cell with two inequivalent Ga sites and three inequivalent O sites. Half the Gallium atoms are in Ga(I) sites which form slightly distorted tetrahedra with four O ions and the other half are in Ga(II) sites which form highly distorted octahedra with six O ions [12].

In view of this rich variety of properties and applications it appears worthwhile to study the surface electronic structure of β-Ga_2O_3. While there is a large body of surface science literature on thin metal oxides films, very few single crystal oxides surfaces have been studied. This is due to a number of obstacles. Among these obstacles, are the difficulties in preparing high purity single crystals and substrates for homoepitaxy, which also limits the attainable progress in device production. Furthermore, the technical difficulty of applying electron-based techniques such as scanning tunneling microscopy (STM) and angle-resolved photoemission spectroscopy (ARPES) to bulk oxides is caused by charging effects arising from the low conductivity. Surface morphology and electronic structure of Ga_2O_3 (100) has been studied with STM, LEED and ARPES on samples prepared by high current annealing, where small terraces were observed and partial correspondence to theoretical band structures has been reported [13]. Thin films obtained by oxidizing CoGa have been studied with STM and low-energy electron diffraction (LEED) [14,15] however, atomic resolution information on single crystal Ga_2O_3 has not been reported. A recent study on β-Ga_2O_3 [16] by ARPES and DFT along Γ-0.5b^* and Γ-0.5c^* directions found a good matching of the experimental band structure with advanced density functional theory calculations. In [16] a slightly smaller indirect band gap of 4.83 eV, with the valence-band maximum (VBM) located slightly away from the M symmetry point has been obtained.

In this paper, we have studied the surface electronic structure of β-Ga_2O_3 along Γ-Z and Γ-M directions by means of ARPES. The electronic band structure presented along the high symmetry lines in the BZ is discussed and compared with density functional theory calculations employing hybrid functionals and projector augmented wave (PAW) potentials [17]. The temperature dependence of the band gap (E_g) of β-Ga_2O_3 determined from ARPES measurements has been studied.

2. Experimental

High resolution photoemission was performed at room temperature on the 5-m-normal incidence monochromator of the beamline BEST with a SES2002 analyzer utilizing the radiation of BESSY II in the photon energy range from 20 eV to 39 eV. An energy resolution of 20 meV and angle resolution of 0.1° was found sufficient to resolve the essential details. The investigated samples were prepared from β-Ga_2O_3 bulk single crystals grown by the Czochralski method using a dynamic growth atmosphere to control partial pressures of volatile species of Ga_2O_3 [2].

3. Sample characterization

β-Ga_2O_3 (100) planes were characterized prior to the measurements by several surface techniques, such as LEED, STM and Laue diffraction. Low energy electron diffraction is used as a standard technique to probe the crystallographic quality of the crystal surface. The sample is cleaved in UHV directly before doing the LEED measurement. The LEED pattern of the β-Ga_2O_3 (100) surface taken at E_{kin} = 188 eV is shown in figure (1a). The LEED picture shows a perfect rectangular lattice and confirms the high quality of the β-Ga_2O_3 crystals. The STM results are shown in figure (1c,1d). Besides the smooth surface observed in STM there are dark spots visible on the surface. These are usually round in shape and are irregularly distributed over the entire surface. They are much smaller than the described terraces in [13]. When the voltage between tip and sample is reversed one sees the same pattern as shown in figure (1c,1d). The origin of the spots is up to now unknown. Figure (1b) shows the Laue diffraction picture. This picture was measured in order to determine the symmetry directions of the (100) surface Brillouin zone. Point contacts of molten tin were fabricated on the backside of the crystals by high voltage yielding good Ohmic contact. The possible charging was checked by applying different photon intensities in the photoemission experiment as shown in figure 2. Absolutely no shift of the spectra was observed, therewith excluding any charging of the sample

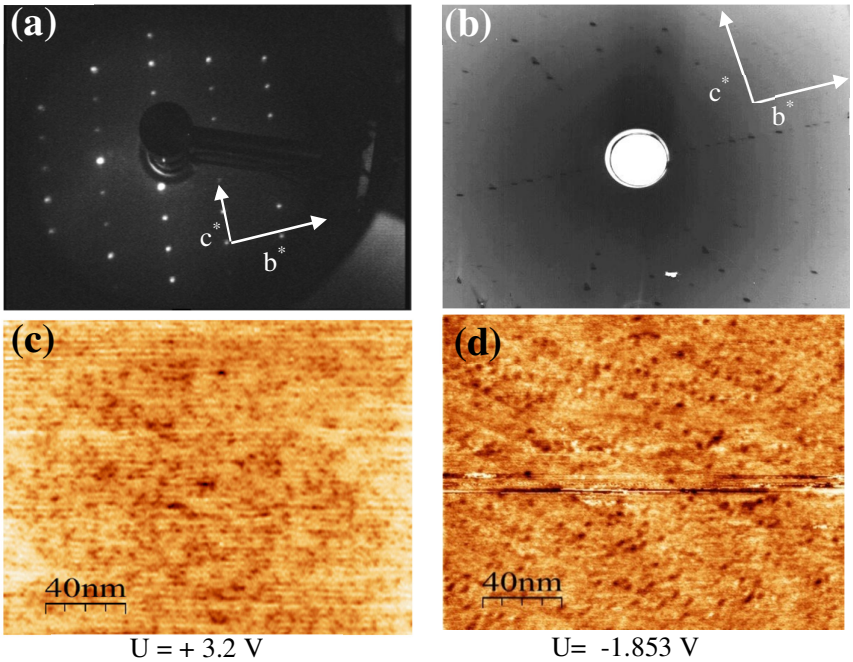

Figure 1. (a), (b) LEED pattern at E_{kin} = 188 eV and Laue picture of the (100)-surface of the β-Ga_2O_3 single crystal. The symmetry directions b* and c* of (100)-surface Brillouin zone are indicated in the LEED and Laue pictures. (c), (d) STM pictures of β-Ga_2O_3 (100)-surface over an area of 200 nm x 200 nm at different potentials between the tip and the sample.

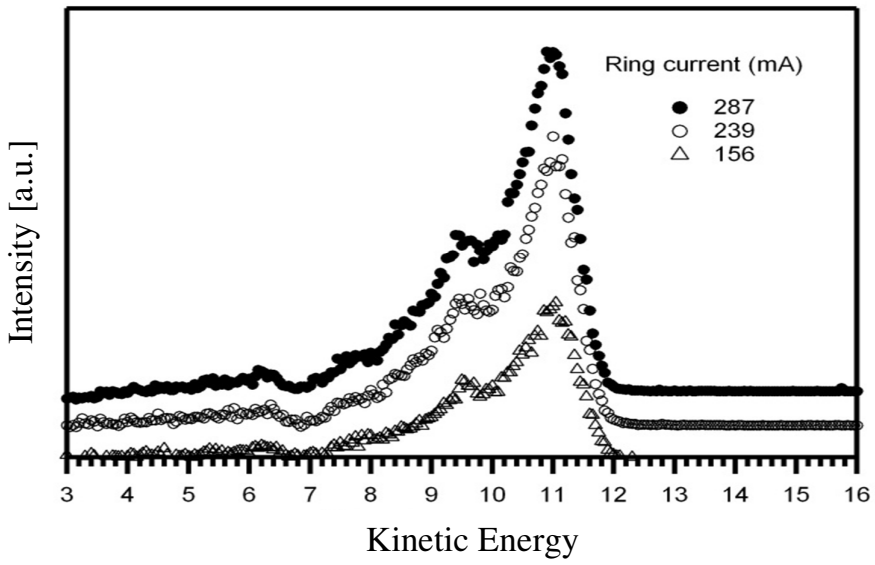

Figure 2. Series of valence band spectra measured at different ring currents at BESSY in order to test the charging effect of the sample.

4. Results and discussion

4.1. The valence band structure along the normal direction (a*):
Measurements performed near normal emission along the a* reciprocal line of the Brillouin zone (the BZ is shown in [16]) of base centered monoclinic β-Ga_2O_3 are shown in figure 3. A series of spectra were taken from 20 eV to 39 eV photon energy in order to determine the exact location of the Γ- point in the BZ. One observes a number of bands with the most prominent feature marked by solid dots. Furthermore, the valence bands at higher binding energies become more pronounced around 30 eV photon energy. Also one can observe clear symmetry of the dispersion around this energy. Thus the Γ-point (the center of the BZ) is at 30 eV.

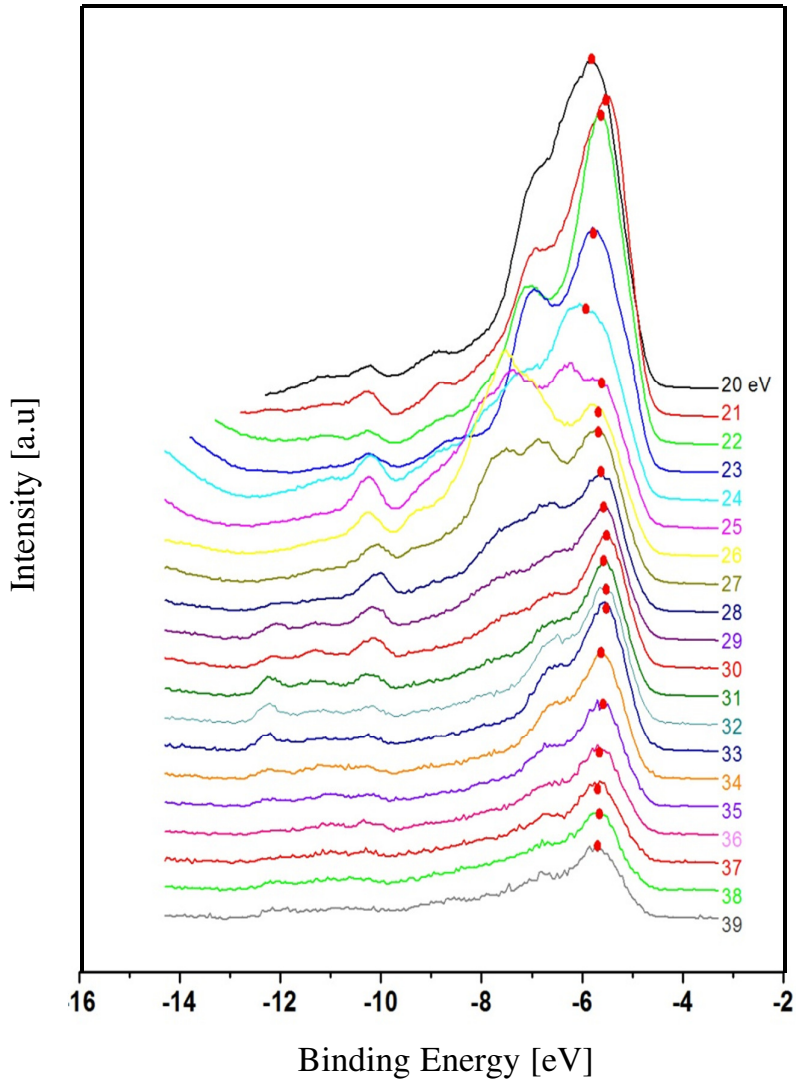

Figure 3. Series of valence band photoemission spectra normal to the cleavage plane of the (100) surface of β-Ga_2O_3 single crystals taken with photon energies from 20 to 39 eV.

Figure (4a,4b) show the photoemission spectrum at the Γ-point and the valence band density of states of β-Ga_2O_3 calculated by density functional theory employing hybrid functionals and projector augmented wave (PAW) potentials [18]. The EDC at the Γ-point in figure (4a) shows many bands from -12.27 to -4.9 eV. This observation confirms the high quality of β-Ga_2O_3 single crystals that have n-type conductivity. One can also observe high intensity bands at lower binding energies than that appearing at higher binding energies. This is in a good agreement with the calculated density of states shown in figure (4b).

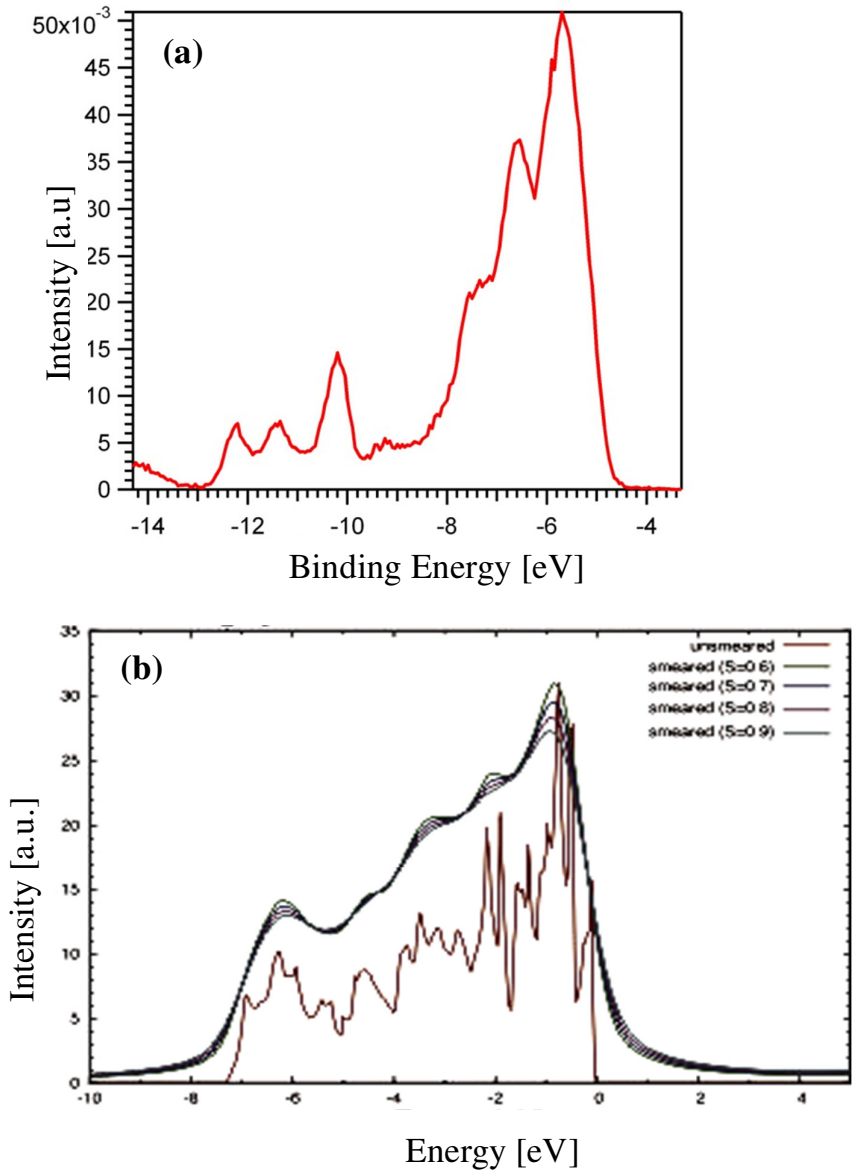

Figure 4. (a) EDC at the Γ-point in the Brillouin zone of β-Ga_2O_3. (b) The valence band density of states of β-Ga_2O_3 calculated by DFT [18].

4.2. The valence band structure along the parallel directions:
From the Γ-point the dispersion relations are studied along the Γ-Z and A-M directions of the Brillouin zone, shown in figure 5. At the Γ-point one finds bands at -12.27, -11.50, and -10.00 eV which show clear k-dispersion. Less intensive bands appear below and above -9 eV and many bands between -4.9 and -8 eV appear as one wide band. The bands near the bottom of the valence band at -12.27 and -10.00 eV come together at 0.5b* in b* direction. The bands at lower binding energy show minor dispersion and high intensity, while the deeper lying bands reveal more dispersion. In the A-M direction the width of the whole valence band is smaller than the width at the Γ-point, where the first band at higher binding energy is at -11.5 eV. Figure 6 compares the experimentally determined bands from Γ to Z and from Γ to M with DFT results [17]. In the Γ- Z and Γ-M directions the band

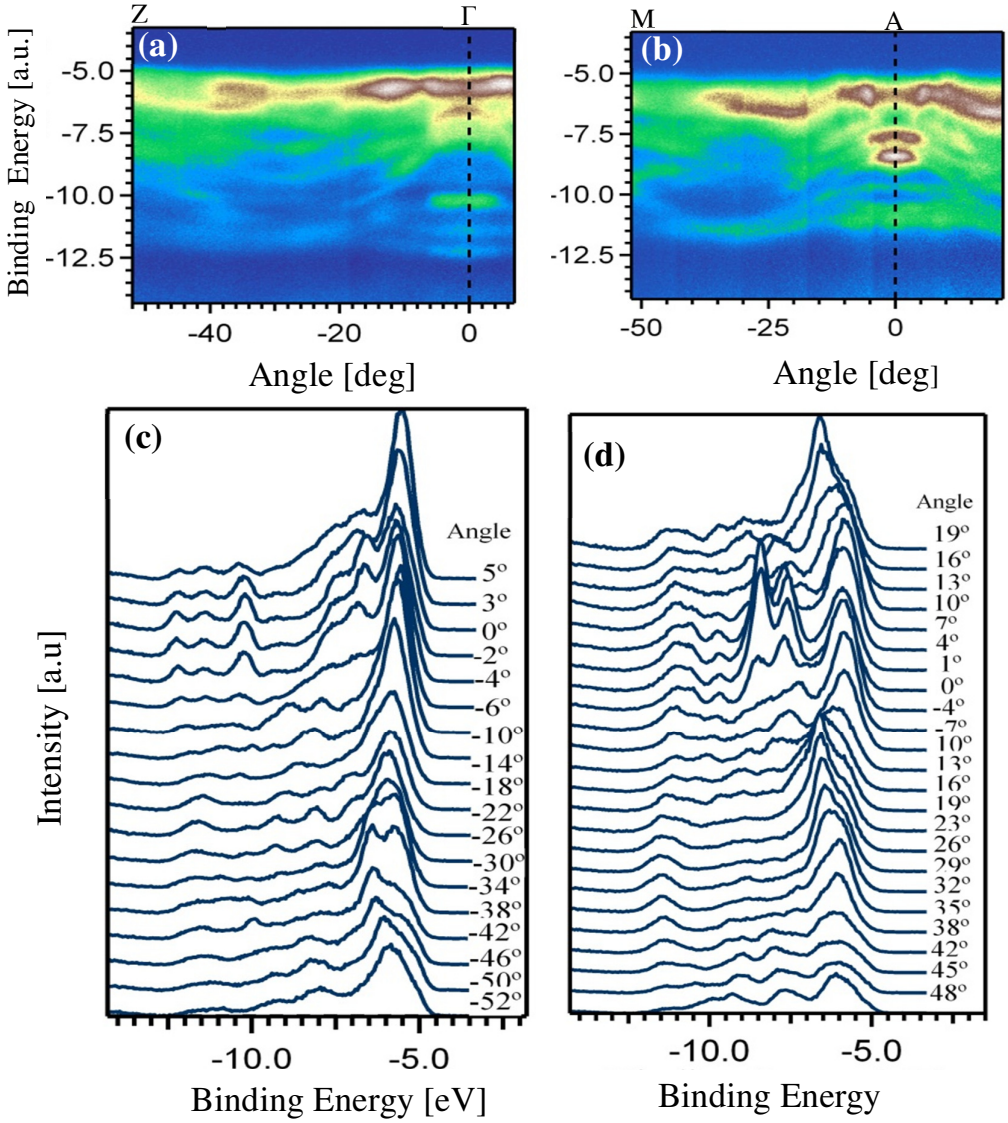

Figure 5. (a), (b) (Intensity map) Experimental band structure along the high symmetry directions Γ-Z and A-M directions of the (100)-surface of β-Ga_2O_3. (c), (d) The corresponding EDC series taken along Γ-Z and A-M for different emission angles.

dispersions show almost excellent agreement with the calculated results. One observes also in the Γ-M symmetry direction a maximum in the valence-band near the M symmetry point. This agrees with the theoretical calculations [16] where an indirect band gap with the valence-band maximum (VBM) located slightly away from the M symmetry point was obtained. In figure (6b) from the Fermi energy down to -4.9 eV binding energy no states appear in the energy gap. This was further checked by scanning this range for a long time without observing any intensity. Since in n-type crystals with the actual electron density of n = 3.5 x 10^{17} cm^{-3} the conduction band is pinned near E_F, the value of 4.9 eV represents within 100 meV the gap value which is in close the value of the optical energy gap of 4.8 eV [19].

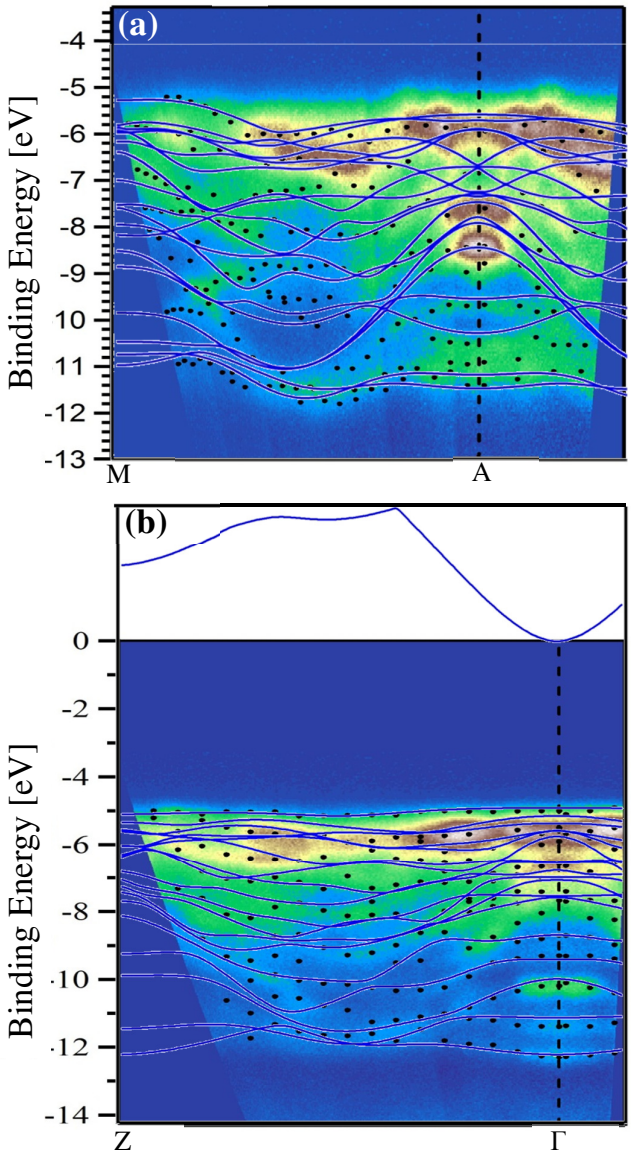

Figure 6. (a), (b) Experimental band structure of β-Ga_2O_3 along the A-M and Γ-Z directions of the Brillouin zone. Black dots show the experimental bands derived from a fit procedure to the spectra. Calculated band structures along Γ-Z and A-M are overlaid on the experimental band structure for comparison.

4.3. The temperature dependence of the band gap (E_g) of β-Ga_2O_3:
Figure (7a) shows a series of photoemission spectra at the Γ-point taken at different temperatures from 300 to 20K. It is observed from these measurements that the photoemission intensity increases with decreasing temperature and the valence bands become much more pronounced and sharper at lower temperatures. The energy band gap determined by linear extrapolations of the valence band maximum shown, in figure (7b), is plotted as a function of the temperature in figure (7c). One can see in figure (7c) that the energy gap decreases with increasing the temperature. This change of the energy gap with temperature is most probably due to electron-phonon interactions [20] that can cause a decreasing band gap of semiconductors with increasing temperature.

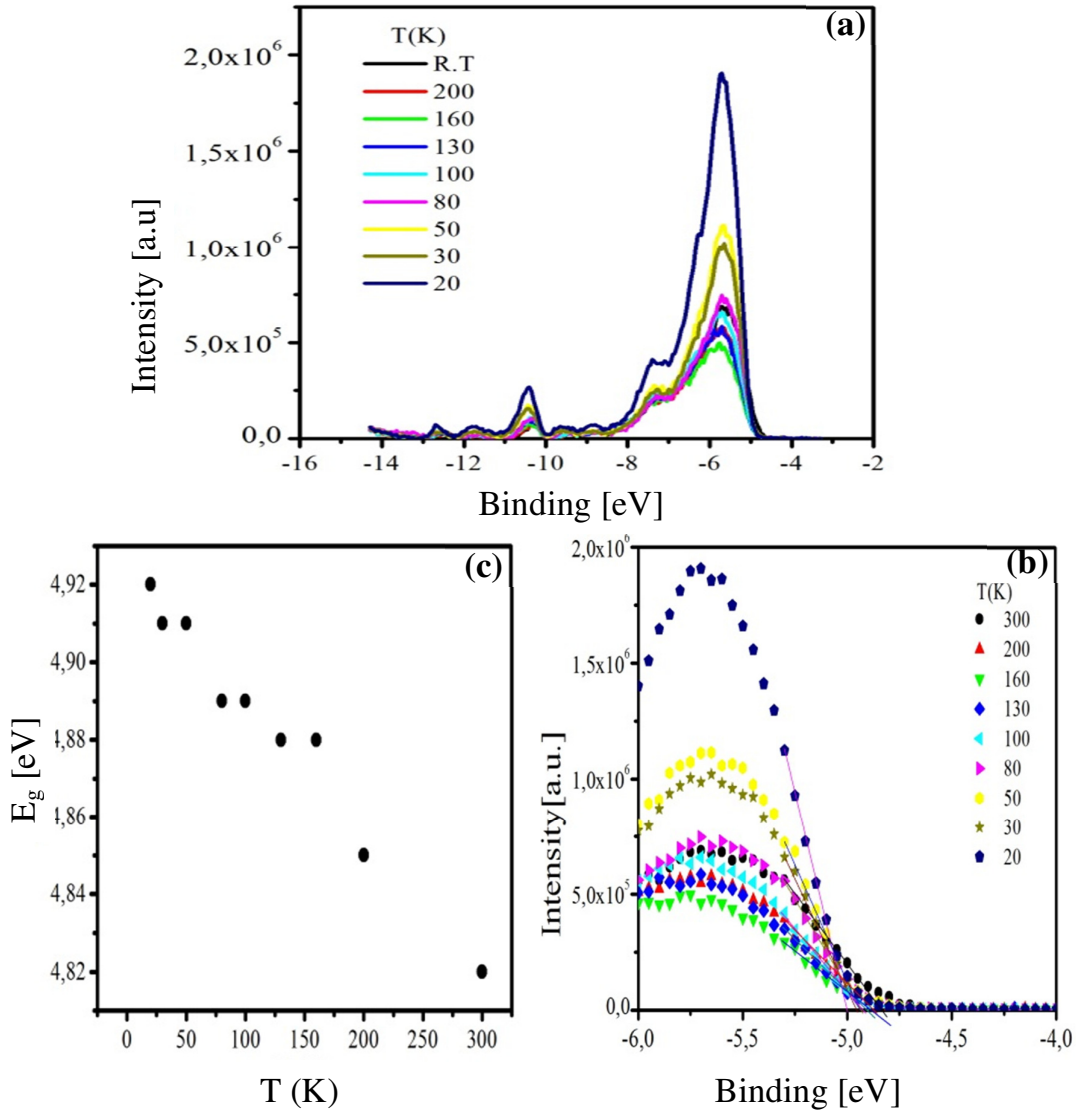

Figure 7. (a) EDCs at the Γ -point taken at different temperatures. (b) The linear extrapolations used to determine the separation between valence band maximum and the Fermi level. (c) Energy band gap (E_g) of β-Ga_2O_3 as a function of the temperature.

5. Conclusion

The (100) cleavage plane of n-type β-Ga_2O_3 grown by the Czochralski method gives a surface of high perfection as became observable in STM, LEED, and ARPES. Comparison of ARPES with the band structure from a DFT calculation shows almost excellent agreement along the Γ-Z and A-M directions of the Brillouin zone. The energy gap of β-Ga_2O_3 decreases with increasing temperature typically due to electron-phonon interactions.

Acknowledgments

This work has been in part conducted at BESSY. We thank the staff for support and in particular Dr. G. Reichardt. Mansour Mohamed thanks Dr. Klaus Irmscher and Mr. Pietsch from IKZ for the valuable help in making Ohmic contact for the samples, the Ministry of Higher Education of Egypt and Assuit University. This work is supported by the DFG (German Research Foundation) under project No. MA2371/8-1.

References

[1] Passlack M, Schubert E F, Hobson W S, Hong M, Moriya N, Chu S N G, Konstadinidis K, Mannaerts J P, Schnoes M L and Zydzik G J 1995 *J. Appl. Phys* **77** 686
[2] Tippins H H 1965 *Phys. Rev.***140** 316
[3] Ueda N, Hosono H, Waseda R and Kawazoe H 1997 *Appl. Phys. Lett.* **70** 3561
[4] Lorentz M R, Woods J F and Gambino R J 1967 *J. Phys. Chem Solids* **28** 403
[5] Harwig T, Wubs G J and Dirksen G J 1976 *Solid State Commun.* **18** 1223
[6] Lorenz M R, Gambino J F W R J 1967 *J. Phys. Chem. Solids* **28** 403
[7] Freisher M and Meixner H *1991 Sens. Actuators B* **4** 437
[8] Roy R, Hill V G and Osborn E F 1952 *J. Am. Chem. Soc.* **74** 719
[9] Roy R, Hill V G and Osborn E F 1953 *Ind. Eng. Chem* **45** 819
[10] Geller S 1960 *J. Chem.Phys.* **33** 676
[11] Geller S 1977 J. *Solid State Chem.* **20** 209
[12] V.M. Bermudez 2006 *Chem. Phys.* **323** 193
[13] Lovejoy T C, Yitamben E N, Shamir N, Morales J, Villora E G, Shimamura K,Zheng S, Ohuchi F S and Olmstead M A 2009 *Appl. Phys. Lett.* **94** 081906
[14] Eumann M, Schmitz G, and Franchy R 1998 *Appl. Phys. Lett.* **72** 3440
[15] Schmitz G, Grassmann P and Franchy R 1998 *J. Appl. Phys.* **83** 2533
[16] Mohamed M, Janowitz C, Unger I, Manzke R, Galazka Z, Uecker R, Fornari R, Weber J R, Varley J B and Van de Walle C G 2010 *Appl. Phys. Lett.* **97** 211903
[17] Varley J B, Weber J R, Janotti A and Van de Walle C G 2010 Appl. Phys. Lett. **97** 142106
[18] Weber J R 2010 *priv. commun.*
[19] Orita M, Ohta H, Hirano M and Hosono H 2000 *Appl. Phys. Lett.* **77** 4166
[20] Manoogian A and Woolley J C 1984 *Can. J. Phys.* **62** 285